Numerical Simulation of an Electrochemical Flow Cell with V-Shape Channel Geometry

Nadiia Kulyk,[a,z] Serhiy Cherevko,[a] Michael Auinger,[a,b,c,*] Claudius Laska,[a] and Karl J. J. Mayrhofer[a,*,z]

[a]*Department of Interface Chemistry and Surface Engineering, Max-Planck-Institut für Eisenforschung GmbH, 40237 Düsseldorf, Germany*
[b]*University of Warwick, Coventry CV4 7AL, United Kingdom*
[c]*InnovMath, A-4632 Pichl bei Wels, Austria*

The electrolyte flow profile and reactive species concentration distribution are calculated for a Scanning Flow Cell (SFC) by means of finite element method numerical calculation using COMSOL Multiphysics software. In case of a simple one-step reaction with kinetic parameters close to those of the oxygen reduction reaction the applicability of conventional Koutecky-Levich (KL) analysis for the kinetic current calculations is proved. In addition, the influence of the cell geometry, particularly the angle between inlet and outlet tubes and the tube diameter, is investigated to guide the further optimization of the method. The applicability of the kinetic analysis is demonstrated experimentally on the example of oxygen reduction reaction.
 [DOI: 10.1149/2.0261512jes] All rights reserved.

Manuscript submitted April 9, 2015; revised manuscript received August 18, 2015. Published August 31, 2015.

For several decades the Rotating Disk Electrode (RDE) has been the standard tool for investigation of electrochemical reactions under defined transport of educts and products to and from the electrode surface, respectively. The major advantage of this approach is the straightforward, well controllable mass transport, which can even be estimated analytically and which leads to nearly uniformity of the local current density over the whole electrode area.[1,2] Thus it enables the exact determination of fundamental kinetic parameters and even pathways of several electrocatalytic reactions independent of electrode geometry, which provides an excellent basis for the development of electrochemical technologies. However, when considering the enormous parameter space spanned by the amounts of electrode materials, electrolyte compositions and operational conditions, a drawback of the RDE and comparable batch investigation techniques are the complexity and the time consumption of the sample and the cell preparation and exchange. Considering all of this, fast and fully automated measurement methods for the reliable determination of kinetic parameters for electrocatalytic reactions under various conditions would be a great advancement for fundamental studies.

The Scanning Flow cell (SFC) is an advanced electrochemical technique that extends the concept of the channel electrode[3] by a "high-throughput" screening capability of previously described Scanning Droplet Cells.[4,5] In our group it has become a major tool for investigations of electrocatalysts, in particular of the stability for some important reactions such as the oxygen reduction reaction (ORR), the oxygen evolution reaction (OER), or the carbon dioxide reduction, metal corrosion and de-alloying,[6–11] circumventing some the above described shortcomings of batch electrochemical approaches.

A number of droplet and flow cells have been presented so far in literature. Most of them aim to perform chemical, bio-chemical and/or electrochemical events at the targeted surface, as well as electrochemical mapping, and make use of probe tips with sizes ranging from one to hundreds of μm.[4,5,12–18] The limitations in interpretation of the electrochemical transients obtained with microelectrochemical cells have been thoroughly studied by Birbilis et al.[19] Moreover, one has to note that electrocatalysts investigations demand a well-controlled flow and diffusion profile of the electrolyte in the vicinity of the electrode and the possibility of kinetic parameters determination, rather than a miniaturization of the droplet cell tips. Thus, cells with openings sizes of the order of 1 mm are a compromise between miniaturization and controllability and robustness of production. Some of such cells have been presented and analyzed by Kollender et al.[20]

The main feature of the SFC is a couple of intersecting channels drilled in a polycarbonate block, which form an elliptical opening at the bottom of the cell body (see Figure 1). A silicone gasket, 100–150 μm thick and with shape and dimensions of the electrode opening, may be attached to the opening to avoid electrolyte leakage in the contact mode. The cell is typically mounted in a fixed, hanging position on a force sensor, which can measure the force applied to the cell body when pressed against the working electrode (WE) surface. A peristaltic pump is utilized to pump the electrolyte from a gas-purged reservoir through tubes connected to the channels of the cell, creating a defined convection profile that can be controlled via the pump rate. The reference and the counter electrode can be placed directly into the channels of the cell, while the WE is placed directly underneath the elliptical opening onto an automated xyz-positioning stage. In non-contact mode, the WE is more than 500 μm away from the elliptical opening at the bottom of the cell and is thus not in contact with the hanging meniscus, established by the electrolyte flowing through the cell channels. When the WE is approached to the bottom of the cell, the electrolyte wets the surface and thereby closes the three-electrode circuit with the counter and reference electrodes in the channels. The

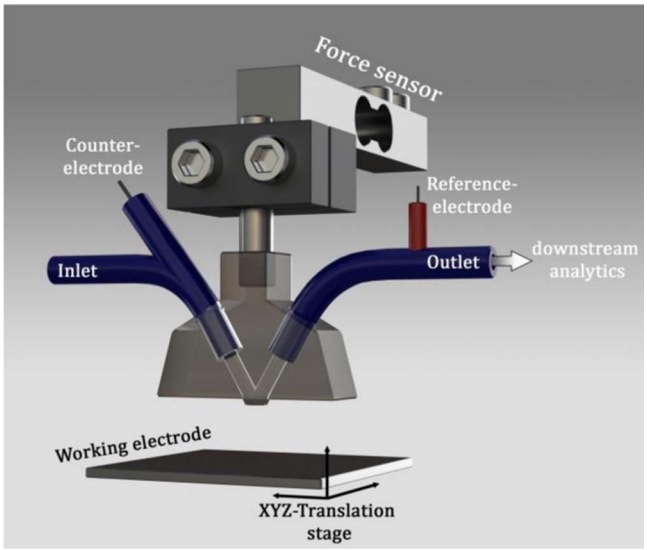

Figure 1. Sketch of the Scanning Flow Cell (SFC). The dimensions of the SFC parts are adjusted for clarity of presentation.

*Electrochemical Society Active Member.
[z]E-mail: kulyk@mpie.de; mayrhofer@mpie.de

WE area in this contact mode is defined precisely by the cell opening and the silicone gasket attached.[9] As a consequence, electrochemical studies can be performed in the confined region of the cell opening as in a classical channel electrode, with the advantage that the position on the sample can be readily exchanged. In addition, since it is a flow-type cell, it enables facile coupling with downstream analysis or even spectrometry.[8–11] The system is also highly versatile due to its modular design and coupling possibilities and can therefore easily be tailored to suit specific requirements.

While the SFC technique has already proven its high potential for various electrochemical screening investigations, the applicability of data analysis by conventional approaches as used for other defined kinetic studies in electrochemistry has not yet been fully proven. Particularly, the accuracy of the Koutecky-Levich (KL) analysis and the Levich equation for the determination of the kinetic current and the limiting current, respectively, has not been scrutinized.[9] Therefore, in this work a numerical study of the flow profile, the concentration profile and the potential-current dependencies is provided for SFCs of different geometries for a simple irreversible reaction. As a result the application of a KL-type analysis is justified, and the accuracy for the determination of kinetics is estimated.

Theoretical Model

The Koutecky-Levich equation was originally developed for the case of a simple irreversible first-order faradaic reaction, involving solution phase redox species on a uniformly-accessible electrode. The only experimental electrochemical method satisfying this condition so far is the RDE.[2] In this case plots of the reciprocal steady-state current (i), measured at a constant overpotential and different rotation rates are linear with respect to the corresponding reciprocal diffusion limiting current (i_{lim}) with an intercept equal to the reciprocal kinetic current (i_{kin}):

$$\frac{1}{i} = \frac{1}{i_{kin}} + \frac{1}{i_{lim}} \qquad [1]$$

The KL equation was also applied to channel electrodes, despite the expected deviation from the ideal case of a uniform current density distribution.[21] Later, Scherson et al. showed analytically that a KL-type relation exists also for the channel electrode for small numbers of $k/v_0^{1/3}$, where k is the reaction rate constant and v_0 is the fluid flow velocity in the center of the channel.[22] However, unlike in the classical KL plot for RDE, the slope is about 6% smaller than unity and slowly increases for larger $k/v_0^{1/3}$, when the current becomes diffusion limited.

Cell geometry.— The Scanning Flow Cells consists of a polycarbonate block in which two intersecting channels with circular cross-sections are drilled.[9] The channels form an elliptical opening at the intersection that is pressed onto a metal plate serving as a working electrode. The flow channels of the cell can be effectively represented for numerical simulations by the scheme shown in Figure 2, where the inlet, the outlet and the electrode surface are indicated. The angle between the channels can be adjusted during the mechanical manufacturing of the cell, which can be performed with a precision of 2 μm. In this study a 60° angle SFC was investigated unless otherwise specified (in the section Influence of the cell geometry). The opening plane that is in contact with the working electrode surface was defined as follows. A plane was drawn through the point where the cylinder axes intersect (see Figure 2), normal to the plane defined by these two axes and parallel to the WE surface. Thus, the opening plane behaves like a cut through a single cylinder, resulting in an elliptic electrode contact area with one length equal to the cylinder diameter and the other one corresponding to $r/\cos(\alpha/2)$ - with α being the angle between the channels and r being the channel radius. The area of the electrode surface is then $\pi r^2/\cos(\alpha/2)$.

The channel diameters were set to be 1 mm for the simulations unless otherwise specified (in the section Influence of the cell geometry), which defines the area of the elliptical opening and the working electrode in contact to be 0.897 mm^2 as calculated by the software.

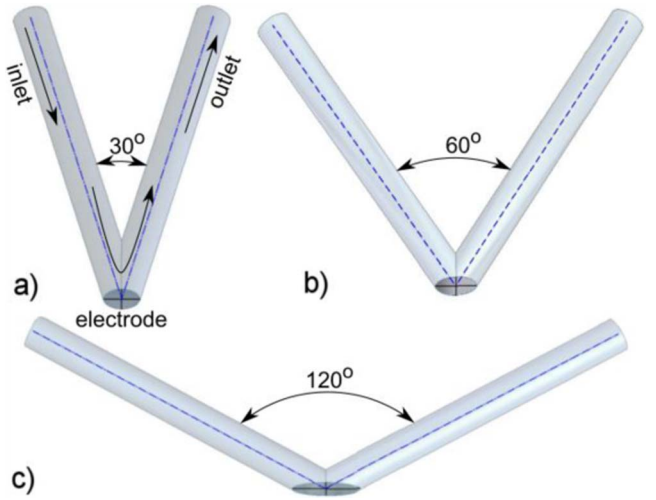

Figure 2. Scheme of the Scanning Flow Cell channels utilized for numerical simulations with an angle of a) 30°, b) 60° and c) 120° between the intersecting inlet and outlet channels. The channel axes are shown; the electrode plane is drawn through the intersection of the two axes of the channels.

Governing equations.— The electrolyte flow profile was calculated using Navier-Stokes equation:[23]

$$\rho\frac{\partial \mathbf{u}}{\partial t} + \rho\left(\mathbf{u}\cdot\nabla\right)\mathbf{u} = \nabla\cdot\left[-\mathrm{p}\mathbf{I} + \mu\left(\nabla\mathbf{u} + (\nabla\mathbf{u})^T\right)\right] + \mathbf{F}, \qquad [2]$$

And the additional condition for incompressible media:

$$\nabla\cdot\mathbf{u} = 0, \qquad [3]$$

Where $\mathbf{u}$ is the velocity field, t is time, ρ is the solution density, p is the pressure, μ is the solution viscosity, $\mathbf{I}$ is the identity matrix, and $\mathbf{F}$ is the external force field. Assuming an established, time independent flow profile ($\frac{\partial \mathbf{u}}{\partial t} = 0$) and negligible external force ($\mathbf{F} = 0$), we arrive to a steady-state equation that was used throughout the calculations:

$$\rho\left(\mathbf{u}\cdot\nabla\right)\mathbf{u} = \nabla\cdot\left[-\mathrm{p}\mathbf{I} + \mu\left(\nabla\mathbf{u} + (\nabla\mathbf{u})^T\right)\right]. \qquad [4]$$

The flow was considered laminar in all cases since the Reynolds number within the cell at the highest flow rate varied only between 0 and 3.

The concentration field of reactive species was calculated using the Nernst-Planck equation without the electric field migration term:[24]

$$\frac{\partial \mathrm{c}}{\partial t} + \mathbf{u}\cdot\nabla\mathrm{c} = \nabla\cdot(\mathrm{D}\nabla\mathrm{c}) + \mathrm{r}, \qquad [5]$$

Where c is the concentration of reactive species, $\mathbf{u}$ is the velocity field, D is the diffusion coefficient and r is the homogeneous reaction rate. Again we assume a steady-state regime ($\frac{\partial \mathbf{c}}{\partial t} = 0$) and absence of homogenous reactions ($\mathrm{r} = 0$):

$$\mathbf{u}\cdot\nabla\mathrm{c} = \nabla\cdot(\mathrm{D}\nabla\mathrm{c}). \qquad [6]$$

Boundary conditions.— In the convection part of the model, the no-slip condition (no velocity difference between the wall and the fluid closest to the wall) was applied at the walls of the cell and at the electrode surface. At the inlet, the laminar flow boundary conditions were applied with a given average velocity and the velocity on edges constrained to zero to match the no-slip conditions on the walls. At the outlet the pressure was defined to be close to atmospheric (10^5 Pa).

For the mass transport equations, the inflow concentration was given as an inlet boundary condition; the outflow condition was chosen for the outlet boundary and the no-flux condition was used at the cell

walls. At the electrode surface, the flux of reactive species was defined according to the Butler-Volmer (BV) equation in the following form:

$$N = -\frac{i_0}{Fn}\frac{c}{c_\infty}\exp\left(\frac{\alpha F\eta}{RT}\right), \quad [7]$$

Where N is the inward flux of the species, proportional to the current density, i_0 is the exchange current density, c and c_∞ are concentrations of the species in the vicinity of the electrode and at the inlet respectively, α is the symmetry parameter, n is the number of electrons transferred for each reactive ion, F is the Faraday constant, R is the universal gas constant, T is the temperature and η is the electrochemical overpotential.

Simulation details.— All simulations were performed using Finite Element software COMSOL Multiphysics 4.0.[25] The geometry discretization was performed through a two-step procedure. First, the "Free Triangular" meshing was applied to the electrode surface, using custom element size. Second, the "Free Tetrahedral" mesh was built for the rest of the geometry. The maximum element size of the "Free Triangular" mesh was reduced gradually until the calculation result for the current through the electrode became independent of the further refining of the mesh. The parameters of the "Free Tetrahedral" mesh were kept constant and predefined as "extra fine" in the COMSOL Multiphysics interface, except for the element "growth rate". The later one was chosen to be 1.18 instead of predefined 1.35 to ensure the smooth transition between fine meshing of the electrode and more robust meshing of the tubing. The adjustments of the mesh size were done separately for each of the cell geometry.

The equations were solved in their stationary form using the default Solver Sequence. The current through the electrode was calculated through the Surface Integration procedure by integrating the normal total flux value over the electrode surface.

Results and Discussion

Diffusion limited reaction regime.— To demonstrate the applicability of the SFC, a simple irreversible reaction was chosen with kinetic and solution parameters close to the ones corresponding to the ORR (see Table I). Thus, without going into detail on the reaction mechanism itself and by keeping the simulation as simple as possible, only effects of the cell geometry and flow conditions on certain representative potential-current curves are investigated.

In a first attempt the diffusion-limited current regime was examined, where the overpotential was deliberately set high enough to provide conditions for the reactive species concentration near the electrode to be effectively zero. Figure 3a shows the resulting electrolyte velocity distribution within the channels when the average velocity at the inlet is 2 mm s^{-1}, represented by the flow profile in the middle y-z plane of the channel. As long as the convection part of the governing equation does not depend on contributions from diffusion (this is a so called weakly coupled system of partial differential equations (PDE)), the velocity profile in the cell depends only on the cell geometry and the inlet boundary conditions. Thus, the velocity profile can be considered as a representative case that can be used for further

Table I. Calculation parameters.

Parameter	Symbol	Value
Diffusion coefficient	D	1.93×10^{-9} m^2 s^{-1}
Concentration at the inlet	c_∞	1.26 mol m^{-3}
Exchange current density	i_0	10^{-6} A m^{-2}
Symmetry factor	α	0.5
Electrons transferred for each reactive ion	n	4
Temperature	T	297 K
Fluid density	ρ	1000 kg m^{-3}
Dynamic viscosity	υ	1.002e-3 Pa s
Inlet velocity	v	0.02–22 mm s^{-1}

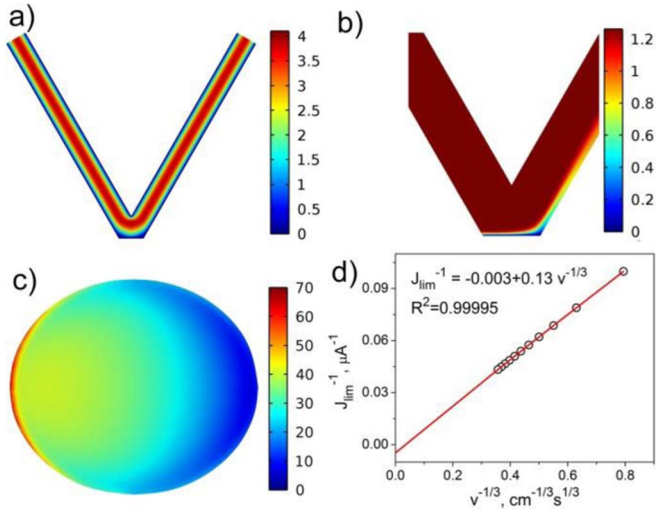

Figure 3. a) Fluid velocity profile in the middle of the channel (representative y-z plane) when the average velocity in the inlet is 2 mm s^{-1}. The scale range is from 0 to 4 mm s^{-1}. b) Concentration distribution in the middle of the channel in the diffusion controlled regime, the inlet velocity is 2 mm s^{-1}. The scale range is from 0 to 1.2 mol m^{-3}. c) Current flux distribution over the electrode surface in the diffusion controlled regime when the inlet velocity is 2 mm s^{-1}. The scale range is from 0 to 70×10^{-6} mol m^{-2} s^{-1}. d) The dependence of reciprocal limiting current on the cubic root of the reciprocal flow rate.

concentration profile calculations in the same geometry at identical flow rates. Note, that Kollender et al.[20] simulated the flow profiles of similar cells using CFD methods and showed similar results, except for the cell referenced as V-shaped SDCM for which a vortex in the outlet tube was found. The V-shaped SDCM differs from the SFC considered here in that the electrode plane was drawn not through the cylinder axis intersection, but at a higher point, thus defining the electrode opening shape as two overlapping ellipses instead of a single ellipse. This geometrical feature most likely causes the mentioned vortex to form in their case.

The concentration profile in the middle of the channel corresponding to the same flow conditions and high overpotentials (limiting current case) is shown on Figure 3b. It becomes clear that the concentration distribution is asymmetrical, perpendicular to the electrode. The reactive species are consumed at the electrode surface during the reaction, leading to lower concentrations close to the electrode and downstream. This is expected due to the electrolyte flow parallel to the surface, which is also observed for standard channel electrodes.[22,26] Interestingly, due to the numerical solution of the mass transport, the full extent of the consumption of the reactive species and its effect on the concentration downstream becomes obvious. Apparently, under the given boundary conditions, the diffusion layer thickness grows along the flow direction and the decrease of concentration close to the lower wall of the channel tube extents quite far toward the outlet. As a consequence, the average concentration of the reactive species is not homogeneous across the channel diameter at the outlet tube, as diffusion is too low for equilibration.

The corresponding normal flux of the species on the electrode (Figure 3c), which is proportional to the current, is not uniform and not symmetric under the given boundary conditions. Actually, the flux ranges from 70×10^{-6} mol m^{-2} s^{-1} at the electrode edge closer to the inlet, which benefits largely from hemispherical diffusion, to around 40×10^{-6} mol m^{-2} s^{-1} in a large part of the center electrode surface, and down to almost 0 at the outlet position of the electrode. This inhomogeneity is expected from the concentration profile in Fig. 3b and the growth of the diffusion layer thickness from inlet to outlet positions. Integrating the flux over the electrode area and multiplying by nF (where F is Faraday constant and $n = 4$ is the number of electrons transferred for each reactive ion), we obtain the expected total current. The dependence of its reciprocal value on the cubic root

of the reciprocal flow rate is shown in Figure 3d. The obtained current data from various flow rates has a linear dependence with an intercept close to zero, which reminds of the corresponding Levich relations for RDE[1] and channel electrodes,[22] and matches experimental results shown in the Supporting Information in Figure S1b. The reciprocal value of current at the intercept, i.e. the limit of measured reciprocal current for an infinitely high inlet velocity, is zero (see Equation 1) and well in line with the notion that the corresponding kinetic current density at this potential in the diffusion limited regime is infinite.[27]

Mixed diffusion/kinetic region.— More interesting from an electrochemical point of view is the overpotential region where the current values are lower than in the diffusion limited case, as it can be utilized to extract kinetic information. In this case the concentration of the reactive species in the vicinity of the electrode can adopt values between 0 (diffusion limited current) and the bulk concentration c_∞ (pure kinetic region). As according to the results from the diffusion limited regime the SFC can be treated as a special case of a channel electrode, the same analytical solution as reported previously can be applied.[22] Note that this approach is expected to cover the similar characteristics of the SFC and regular channel electrodes, like the non-uniformity of the concentration and current profiles and the change of the diffusion layer thickness along the electrode surface. Thus, one should also expect similar polarization curve behavior and ideally the same kinetic quantities for both systems.

Figures 4a and 4b provide a visualization of the concentration and flux profiles at the electrode (inlet velocity 2 mm s^{-1}) for three values

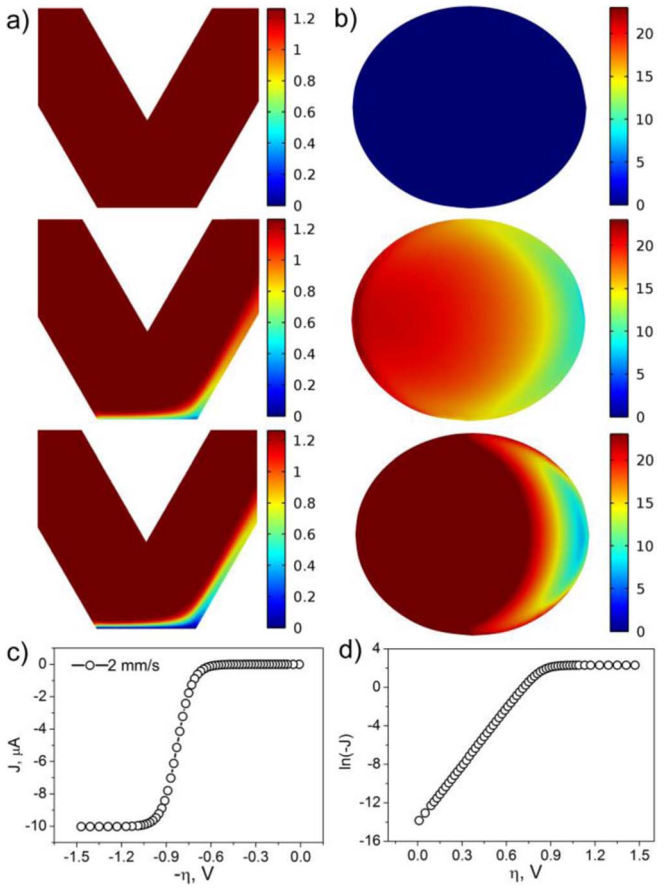

Figure 4. a) Concentration in the middle channel plane and b) flux at the electrode surface for the overpotential values of 0.5 V (upper images), 0.85 V (middle images) and 1.4 V (lower images). The scale range is from 0 to 1.2 mol m^{-3} in a) and from 0 to 20 × 10^{-6} mol $m^{-2}s^{-1}$ in b), and is kept the same in all plots of this figure for comparison reasons. c) Polarization curve and d) corresponding Tafel plot. In all calculations the average inlet flow rate is 2 mm s^{-1}.

of overpotential, one lying in the kinetic region (0.5 V), one in the mixed diffusion/kinetic region (0.85 V) and one in the limiting current region (1.4 V). For clarity all the color scale ranges are kept constant and only the part of the channels close to the electrode is shown. It is clear that in the true kinetic region, the concentration close to the electrode surface is approximately equal to the bulk value. Since the reaction rate is small, no diffusion effects appear and consequently the flux of the species is uniform over the electrode. When the overpotential lies in the mixed diffusion/kinetic region, the situation drastically changes. A diffusion layer with a concentration distribution different from the bulk value appears. The thickness of the diffusion layer changes along the electrode already at these low reaction rates. Significant edge effects start to appear due to hemispherical diffusion and thus the concentration at the electrode becomes non-uniform. In turn, the flux of the species at the electrode is also inhomogeneous and varies by a factor of three.

As already mentioned, in the limiting current region the non-uniform flux reaches a maximum, even though the concentration at the whole electrode is effectively zero.[27] The corresponding polarization curve is shown on Figure 4c. It has a classical shape reminding of the ones obtained usually on RDE or channel electrodes and matches the ones obtained experimentally earlier in our group[9] and the ones shown in the Supporting Information, Figure S1a. The corresponding Tafel plot is shown in Figure 4d.

Diffusion correction.— The conventional analysis of polarization curves under forced convection is performed by utilizing the Koutecky-Levich equation (Eq. 1). It was also shown that for small numbers of $k/v^{1/3}$ and with a correction factor close to unity, the equation holds with high precision for a channel electrode.[22] By simulation of polarization curves for different flow rates, the validity of the approach for the SFC can be investigated.

In Figures 5a, 5b and 5c, we show the polarization curves calculated for three different inflow velocities, the corresponding Tafel plots as well as the plots of kinetic current calculated using Eq. 1. The slope of the linear fit of the kinetic current logarithm corresponds to the value of $\frac{\alpha n F}{RT}$, which is equal to 19.55 in all the calculations. The slopes obtained for the inlet velocity 2, 8 and 16 mm s^{-1} are equal to 19.86, 19.79 and 19.86 correspondingly, which is a match of very high precision. The intercepts that correspond to the logarithm of the exchange current density are also well in line with the value we originally used in the Butler-Volmer equation (−13.9). The same analysis is also applied for the CV curves obtained experimentally for ORR reaction as shown in Supporting Information in Figure S1c. This suggests that independent of the inhomogeneous current density distribution and of the edge effects, the KL equation for a channel electrode can also be reliably used for the SFC.

Influence of the cell geometry.— The manufacturing of the SFC allows the geometry to be varied readily, particularly the angle between the inlet and outlet tubes. The influence of the angle on the performance evaluation and accuracy of the reaction kinetic parameters calculation is simulated in this section. For this purpose SFC cells with three different angles are simulated, namely 30°, 60° and 120°, and their corresponding geometries used for calculations are shown in Figures 2a–2c. The tube length was 10 mm in each case, with a tube diameter of 1 mm, and the resulting contact area of the electrode was 0.8035 mm^2, 0.8967 mm^2 and 1.553 mm^2 respectively. Intuitively, the geometry with the largest angle between the tubes should behave similarly to a standard channel electrode, while the one with the smallest angle rather resembles cells with a vertical channel structure.[23] Although the channel electrode has been described analytically before, no data on current distribution and especially on the applicability of the vertical channel cells for estimating the reaction kinetic parameters via the KL equation is available to the best of our knowledge.

Figures 6a–6c shows the flux distribution over the electrode calculated for the case of an inflow velocity of 2 mm s^{-1} and overpotential

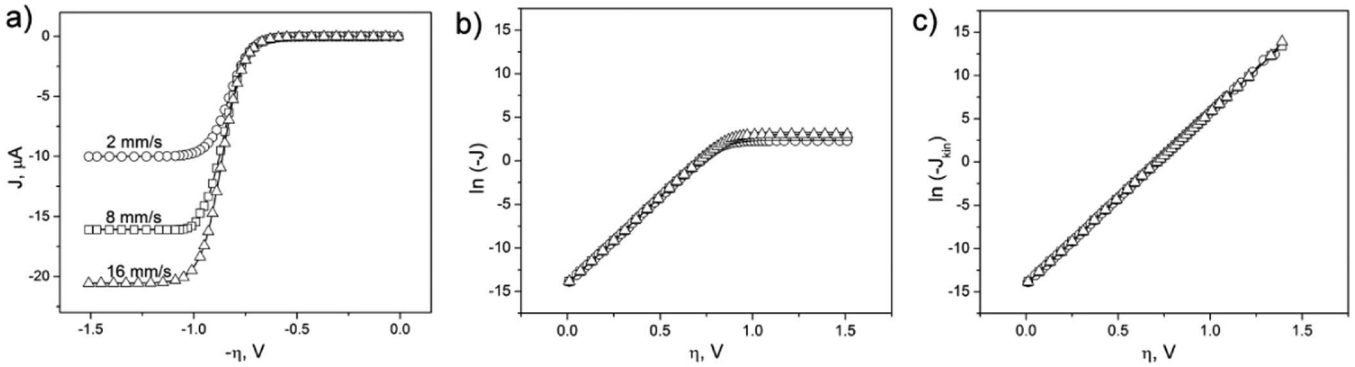

Figure 5. a) Polarization curves calculated for varying inflow velocities as indicated. b) Tafel plots calculated for the polarization curves from a). c) Tafel plots corrected for the diffusion limited current calculated for polarization curves a) using Eq. 1.

of 0.85 V for the three geometries. The color scale range is kept the same for clarity. It is obvious that the cell with a 120° angle provides the highest flux values over the electrode due to more effective convection and lower average diffusion layer thickness. In contrast, the least effective cell is the one with a minimal angle between the tubes. All three cells, however, have a certain asymmetry in the flux distribution in common, with higher flux values on the inlet side (left side). Nevertheless, the Koutecky-Levich type relation holds for all three cells with high accuracy (Figures 6d–6f). The plots of reciprocal J vs. reciprocal J_{lim} are straight lines with the slopes being 0.98, 1.001 and 0.99, and the intercepts being 13.36^{-1} μA^{-1}, 15.68^{-1} μA^{-1} and 26.72^{-1} μA^{-1} respectively. When the reciprocal values of the intercepts are divided by the corresponding electrode surface area (see above), the kinetic current density according to Eq. 1 can be extracted to be 1.66 mA cm^{-2}, 1.75 mA cm^{-2}, 1.72 mA cm^{-2}, respectively. The theoretical current density expected from the BV equation equals 1.65 mA cm^{-2} under the assumption of a homogeneous current distribution. Hence, the accuracy of the kinetic current density calculation for all three cells falls within 6%, showcasing that the approach is feasible for the determination of kinetic parameters with sufficient accuracy for electrochemical systems independent of the angle between the channels.

As, the scanning flow cell often has a gasket (a silicone ring) used to avoid leakage of the electrolyte,[9–11] we additionally performed calculations on its influence on the determination of kinetic parameters. The thickness of such a ring is around 100 μm and its shape replicates the shape of the electrode opening (see Figure S2 in Supporting Information). The KL plot for such a cell with a 100 μm gasket is shown in Figure 7a. One can see that the slope of the plot is very close to unity (0.98) and the intersect is 14.88^{-1} μA^{-1}, which corresponds well to the kinetic current density calculated by BV equation at 0.85 V overpotential (1.65 mA cm^{-2}) and the one calculated for the cell without gasket (Figure 6e).

Note that another possible variation of the cell geometry can be introduced by the channel diameter. A KL plot summarizing the results from the calculations for a cell with 0.1 mm channels is shown on Figure 7b. The flow rate range for this cell was chosen to be 0.2 – 2.2 mm s^{-1}, while for higher flow rates a calculation error occurred due to the high solution velocity gradient. The slope of the KL plot for this cell is also very close to unity (0.99) and the intersept is 0.15^{-1} μA^{-1}, which corresponds to 1.5 mA cm^{-2} kinetic current. The slight increase in kinetic current determination error observed may be due to the more pronounced edge effects as expected.

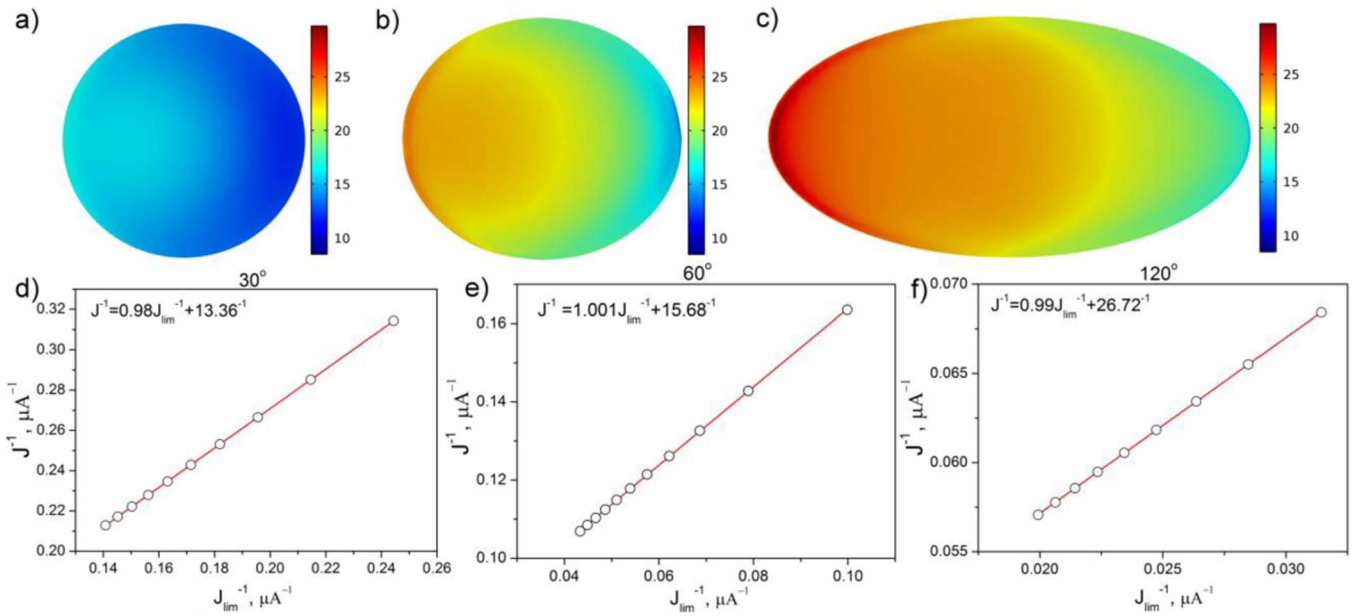

Figure 6. a-c) Flux distribution over the electrode in SFC for the angle between tubes of a) 30°, b) 60°, c) 120°. The inflow velocity is 2 mm s^{-1} and overpotential is 0.85 V for all three geometries. The color scale range is from 0 to 30 × 10^{-6} mol m^{-2} s^{-1}. d-f) Koutecky-Levich plot for the SFC with the angle between tubes d) 30°, e) 60°, f) 120°. The inflow velocity ranges from 2 to 22 mm s^{-1}, the overpotential is 0.85 V.

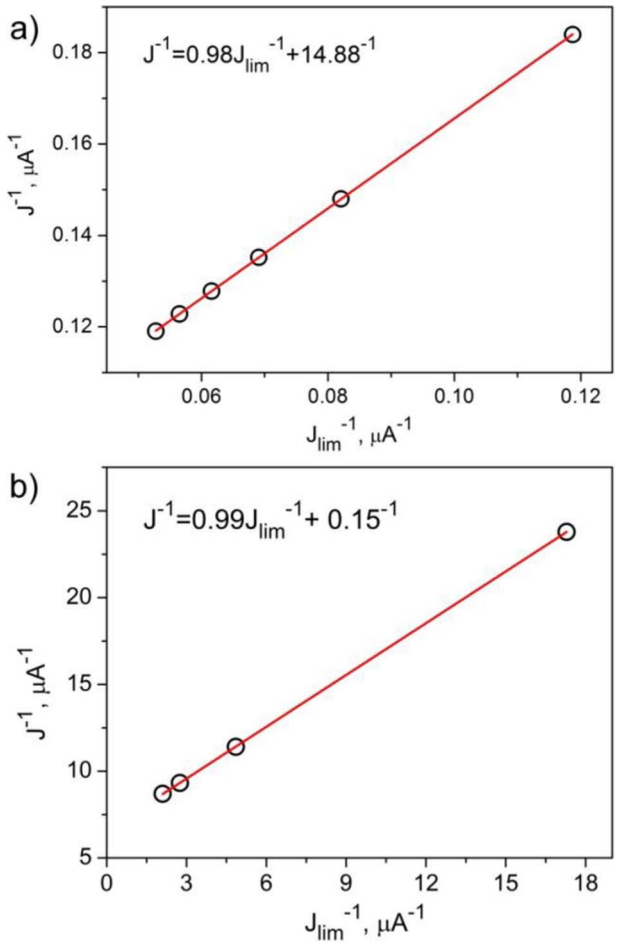

Figure 7. a) KL plot for the SFC with 1 mm tube diameter and a 100 μm gasket. b) KL plot for the SFC with channel diameter of 0.1 mm.

Nevertheless, even for this small opening size the accuracy of 10% is still acceptable.

Limits to the finite element numerical calculations.— Although the modelling already has proven to be very consistent also with regards to different geometries, and thus has confirmed the feasibility of the SFC for kinetic studies, still certain restrictions have to be considered. For instance, it was assumed through all calculations that the flow of electrolyte is laminar. However, turbulences could occur when the Reynolds number Re becomes larger than 2000. Considering $Re = \frac{vD\rho}{\mu}$, the limiting inlet velocity is around 1 m s^{-1}. As this flow speed is two orders of magnitude larger than in our calculations, it is safe to consider the flow as laminar.

Another limit to be considered, as our numerical simulations show, is the deviation from Levich equation that starts to appear when the diffusion layer overlaps or is comparable to the cell channel thickness. This happens for instance when the inlet velocity is smaller than 0.02 mm s^{-1} for the SFC with 1 mm channel diameter, which is however not used in application.

The most restricting assumption in our model is the steady state regime. In real applications (for an example see Supporting Information) a finite scan rate is used for cyclic voltammetry measurements and the system is generally not in steady state. Our experimental data show that for ORR so called "overshooting" exists, when a peak appears in the negative going scan and the current is lower than expected in the positive going scan. This can be however easily circumvented by small scan rates and higher flow rates. Optimal values of the scan rate and flow rate should be found in every case as a compromise between measurement time and accuracy. In our measurements (see Supporting Information) scan rates of 5 mV s^{-1} and 20 mV s^{-1} and flow rate up to 4 mm s^{-1} lead to reasonable estimate of kinetic parameters and linear KL plot. Note that our experimental data demonstrates that at higher scan rates the KL-like relationship still holds but shows a slope strongly deviating from unity.

Finally, although the numerical simulations exhibit no deviation from the KL relation depending on the reaction kinetic rate constant (or on overpotential, see Figure 5c), it has to be considered that only a simple one-step reaction is modelled here, while some deviations may appear in case of more complex multistep reactions, but this is out of scope of the current work.

Conclusions

The applicability of the scanning flow cell for electrochemical measurements has been tested via numerical calculations of Navier-Stokes and mass balance equations, using a finite element method based software. The concentration and current distribution on the electrode is calculated for the case of a simple one-step electrochemical reaction. When the overpotential is high enough and the reaction is not kinetically controlled, the current distribution over the electrode is highly inhomogeneous and the electrode cannot be treated as a uniformly accessible one, as for instance the RDE. Nevertheless, the standard kinetic current extraction procedure involving Koutecky-Levich analysis can be applied. The diffusion limiting current dependence on the electrolyte flow rate is similar to the one calculated for a regular channel electrode, and resembles the dependence of the limiting current on the rotation rate in case of an RDE. The Koutecky-Levich equation applies for the SFC system in the tested flow rate range with a 6% precision; the kinetic current can be extracted by measuring limiting current values and current values in the mixed kinetic region like in case of RDE measurements. The effect of the SFC geometry was examined and shows that smaller angles between inlet and outlet tubes tend to result in smaller average current values for the same overpotentials. While all cells demonstrate highly non-uniform current distribution over the electrode independent from the angle; the accuracy of the Koutecky-Levich analysis does not change significantly with the angle. In contrast, a strong reduction of the channel diameter may affect the accuracy of the kinetic analysis and lead to misinterpretation of the data. Experimental investigations of the SFC performance (see *Supporting Information*) show that when the system is in a regime close to steady state, standard kinetic analysis can be applied to extract kinetic parameters of the reaction, as suggested by modelling. All this confirms that the SFC has great potential in modern electrochemical research, particularly for mass transport independent, automated kinetic studies in a high throughput mode.

Acknowledgments

C.L. acknowledges finacial support from the International Max-Planck Research School IMPRS SurMat. K. M. acknowledges financial support by the DFG over the project MA 4819/4-1.

References

1. V. G. Levich, *Physicochemical hydrodynamics*, Prentice-Hall, 1962.
2. B. Levich, *Discussions of the Faraday Society*, **1**, 37 (1947).
3. J. A. Cooper and R. G. Compton, *Electroanalysis*, **10**, 141 (1998).
4. M. M. Lohrengel, A. Moehring, and M. Pilaski, *Electrochimica Acta*, **47**, 137 (2001).
5. M. M. Lohrengel, C. Rosenkranz, I. Klüppel, A. Moehring, H. Bettermann, B. V. D. Bossche, and J. Deconinck, *Electrochimica Acta*, **49**, 2863 (2004).
6. M. J. Duarte, J. Klemm, S. O. Klemm, K. J. J. Mayrhofer, M. Stratmann, S. Borodin, A. H. Romero, M. Madinehei, D. Crespo, J. Serrano, S. S. A. Gerstl, P. P. Choi, D. Raabe, and F. U. Renner, *Science*, **341**, 372 (2013).
7. J.-P. Grote, A. R. Zeradjanin, S. Cherevko, and K. J. J. Mayrhofer, *Review of Scientific Instruments*, **85**, 104101 (2014).
8. S. O. Klemm, A. A. Topalov, C. A. Laska, and K. J. J. Mayrhofer, *Electrochemistry Communications*, **13**, 1533 (2011).
9. A. K. Schuppert, A. A. Topalov, I. Katsounaros, S. O. Klemm, and K. J. J. Mayrhofer, *Journal of The Electrochemical Society*, **159**, F670 (2012).
10. S. Cherevko, A. Topalov, A. Zeradjanin, G. Keeley, and K. J. Mayrhofer, *Electrocatalysis*, **5**, 235 (2014).

11. S. Cherevko, A. R. Zeradjanin, A. A. Topalov, N. Kulyk, I. Katsounaros, and K. J. J. Mayrhofer, *ChemCatChem*, **6**, 2219 (2014).
12. D. Juncker, H. Schmid, and E. Delamarche, *Nat Mater*, **4**, 622 (2005).
13. D. Momotenko, F. Cortes-Salazar, A. Lesch, G. Wittstock, and H. H. Girault, *Analytical Chemistry*, **83**, 5275 (2011).
14. T. W. Spaine and J. E. Baur, *Analytical Chemistry*, **73**, 930 (2001).
15. C. G. Williams, M. A. Edwards, A. L. Colley, J. V. Macpherson, and P. R. Unwin, *Analytical Chemistry*, **81**, 2486 (2009).
16. G. V. Kaigala, R. D. Lovchik, U. Drechsler, and E. Delamarche, *Langmuir*, **27**, 5686 (2011).
17. N. Ebejer, M. Schnippering, A. W. Colburn, M. A. Edwards, and P. R. Unwin, *Analytical Chemistry*, **82**, 9141 (2010).
18. K. Fushimi, S. Yamamoto, H. Konno, and H. Habazaki, *ChemPhysChem*, **10**, 420 (2009).
19. N. Birbilis, B. N. Padgett, and R. G. Buchheit, *Electrochimica Acta*, **50**, 3536 (2005).
20. J. P. Kollender, M. Voith, S. Schneiderbauer, A. I. Mardare, and A. W. Hassel, *Journal of Electroanalytical Chemistry*, **740**, 53 (2015).
21. N. Wakabayashi, M. Takeichi, M. Itagaki, H. Uchida, and M. Watanabe, *Journal of Electroanalytical Chemistry*, **574**, 339 (2005).
22. D. A. Scherson, Y. V. Tolmachev, Z. Wang, J. Wang, and A. Palencsar, *Electrochemical and Solid-State Letters*, **11**, F1 (2008).
23. A. W. Hassel and M. M. Lohrengel, *Electrochimica Acta*, **42**, 3327 (1997).
24. M. Auinger, I. Katsounaros, J. C. Meier, S. O. Klemm, P. U. Biedermann, A. A. Topalov, M. Rohwerder, and K. J. J. Mayrhofer, *Physical Chemistry Chemical Physics*, **13**, 16384 (2011).
25. E. J. F. Dickinson, H. Ekström, and E. Fontes, *Electrochemistry Communications*, **40**, 71 (2014).
26. Y. V. Tolmachev, Z. Wang, and D. A. Scherson, *Journal of The Electrochemical Society*, **143**, 3160 (1996).
27. A. Bard and L. Faulkner, *Electrochemical Methods: Fundamentals and Applications*, John Wiley & Sons, Inc, 2001.